



HAL
open science

Diurnal concentrations, sources, and cancer risk assessments of 1 PM 2.5 -bound PAHs, NPAHs, and OPAHs in urban, marine and 2 mountain environments

Junmei Zhang, Lingxiao Yang, Abdelwahid S Mellouki, Jianmin Chen, Xiangfeng Chen, Ying Gao, Pan Jiang, Yanyan Li, Hao Yu, Wenxing Wang

► To cite this version:

Junmei Zhang, Lingxiao Yang, Abdelwahid S Mellouki, Jianmin Chen, Xiangfeng Chen, et al.. Diurnal concentrations, sources, and cancer risk assessments of 1 PM 2.5 -bound PAHs, NPAHs, and OPAHs in urban, marine and 2 mountain environments. *Chemosphere*, 2018, 209, pp.147-155. 10.1016/j.chemosphere.2018.06.054 . hal-02459186

HAL Id: hal-02459186

<https://hal.science/hal-02459186>

Submitted on 29 Jan 2020

HAL is a multi-disciplinary open access archive for the deposit and dissemination of scientific research documents, whether they are published or not. The documents may come from teaching and research institutions in France or abroad, or from public or private research centers.

L'archive ouverte pluridisciplinaire **HAL**, est destinée au dépôt et à la diffusion de documents scientifiques de niveau recherche, publiés ou non, émanant des établissements d'enseignement et de recherche français ou étrangers, des laboratoires publics ou privés.

1 **Diurnal concentrations, sources, and cancer risk assessments of**
2 **PM_{2.5}-bound PAHs, NPAHs, and OPAHs in urban, marine and**
3 **mountain environments**

4
5 Junmei Zhang^a, Lingxiao Yang^{a,c,*}, Abdelwahid Mellouki^{a,d}, Jianmin Chen^{b,e},
6 Xiangfeng Chen^f, Ying Gao^b, Pan Jiang^a, Yanyan Li^a, Hao Yu^b, Wenxing Wang^a

7 ^aEnvironment Research Institute, Shandong University, Jinan 250100, China

8 ^bSchool of Environmental Science and Engineering, Shandong University, Jinan
9 250100, China

10 ^cJiangsu Collaborative Innovation Center for Climate Change, China

11 ^dInstitut de Combustion, Aerothermique, Reactivité Environnement (ICARE),
12 CNRS/OSUC, 1C Avenue de la Recherche Scientifique, 45071 Orléans Cedex 02,
13 France

14 ^eShanghai Key Laboratory of Atmospheric Particle Pollution and Prevention
15 (LAP3), Fudan Tyndall Centre, Department of Environmental Science and
16 Engineering, Fudan University, Shanghai 200433, China

17 ^fKey Laboratory for Applied Technology of Sophisticated Analytical Instruments,
18 Shandong Analysis and Test Centre, Qilu University of Technology (Shandong
19 Academy of Sciences), Jinan, Shandong, 250014, P. R. China.

20

21 *Corresponding author. Email: yanglingxiao@sdu.edu.cn

22 Telephone: 86-531-88364896

23 Fax: 86-531-88364896

Abstract

Ambient measurements of PM_{2.5}-bounded polycyclic aromatic hydrocarbons (PAHs), nitro-PAHs (NPAHs), and oxy-PAHs (OPAHs) were conducted during the summer in Jinan, China, an urban site, and at Tuoji island and Mt. Tai, two background locations. 3.5 h and 11.5 h sampling intervals in daytime and nighttime were utilized to research the diurnal variations of PAHs, NPAHs, and OPAHs. The concentrations of PAHs, NPAHs, and OPAHs were highest at the urban site and lowest at the marine site. The diurnal patterns of PAHs and NPAHs at the urban and marine sites were dissimilar to those observed at the mountain site partly due to the influence of the boundary layer. Vehicle emissions at the urban site made a large contribution to high molecular weight PAHs. 1N-PYR and 7N-BaA during morning and night sampling periods in JN were relatively high. Fossil fuel combustion and biomass burning were the main sources for all three sites during the sampling periods. The air masses at the marine and mountain sites were strongly impacted by photo-degradation, and the air masses at the marine site were the most aged. Secondary formation of NPAHs was mainly initiated by OH radicals at all the three sites and was strongest at the marine site. Secondary formation was most efficient during the daytime at the urban and mountain sites and during morning periods at the marine site. The average excess cancer risk from inhalation (ECR) for 70 years' life span at the urban site was much higher than those calculated for the background sites.

Keywords

PAHs, NPAHs, OPAHs, marine and mountain sites, diurnal variations

1. Introduction

Increasing levels of ambient particulate matter (PM) pollution from rapid urbanization and economic development in China have drawn worldwide attention and have substantial adverse effect on human health (Wang et al., 2014). The International Agency for Research on Cancer

53 (IARC) classified PM from outdoor air pollution as carcinogenic to humans in 2013 (Loomis et
54 al., 2013). The toxicity of PM is dependent on the certain chemical components, such as
55 polycyclic Aromatic Hydrocarbons (PAHs) and their derivatives. PAHs are known to be
56 mutagenic, genotoxic, and carcinogenic persistent organic pollutants (Abdel-Shafy and
57 Mansour, 2016; Łuczyński et al., 2005) and are mainly emitted by incomplete combustion of
58 organic materials, such as from coal and biomass burning, vehicle emissions, and industrial
59 processes. NPAHs and OPAHs are nitrated and oxygenated derivatives of PAHs, respectively.
60 Many NPAHs and OPAHs are more toxic than their parent PAHs due to their direct-acting
61 mutagenicity and carcinogenicity (Albinet et al., 2008; Pedersen et al., 2005), and high
62 molecular weight NPAHs and OPAHs generally present a greater hazard to health due to their
63 carcinogenic behavior. NPAHs and OPAHs are not only directly co-emitted with PAHs but also
64 formed through atmospheric photochemical reactions of parent PAHs with OH, NO_x, and O₃
65 radicals (Reisen and Arey, 2005; Jariyasopit et al., 2014). The relative contributions of primary
66 and secondary sources of NPAHs and OPAHs varies greatly between different sampling sites
67 and periods (Kojima et al., 2010; Li et al., 2015).

68 To date, surveys of the concentrations, sources, transformation reactions, and long-distance
69 transport of NPAHs and OPAHs have been carried out in 24 h, monthly, and seasonal sampling
70 periods (Albinet et al., 2007, 2008; Zhuo et al., 2017; Zimmermann et al., 2012), which may be
71 influenced by the sampling artifact mainly including oxidative degradation caused by O₃ within
72 the samplers (Balducci et al., 2018; Liu et al., 2014). Possibly due to the limits of current
73 analytical techniques or the low concentration of NPAHs and OPAHs bounded in PM, shorter
74 temporal sampling resolution measurements studies are scarce. As we know, only a few studies

75 have reported 12 h (Ringuet et al., 2012; Souza et al., 2014), 3 or 4 h (Alam et al., 2015;
76 Tsapakis and Stephanou, 2007), and 3.5 h and 11.5 h time intervals during the daytime and
77 nighttime, respectively (Reisen and Arey, 2005) measurements to analyze the diurnal variation
78 of NPAHs and OPAHs, which were mainly carried out at one or two sampling sites among
79 traffic site, suburban site, rural site, urban site, urban background site and marine background
80 site, and the molecular compositions of NPAHs and OPAHs were different from those in the
81 paper. No research has been found to study the diurnal variation of NPAHs and OPAHs under
82 mountain atmosphere conditions by short time intervals, let alone the detailed comparison
83 among mountain, marine and urban sampling sites. Less resolved measurements are subjected
84 to substantial disadvantages when attempting to understand the physical and chemical processes
85 (e.g., secondary formation) in the atmosphere (Ringuet et al., 2012). Shorter sampling periods
86 are more conducive to exploring the fate and governing factors of NPAHs and OPAHs (Elorduy
87 et al., 2016).

88 The concentrations and physicochemical properties of chemicals present in the
89 atmospheric environment vary by sampling regions due to many factors, such as differences in
90 population density, life style, or meteorological conditions (Seinfeld et al., 2004; Wang et al.,
91 2012). Therefore, the molecular components and levels of PAHs, NPAHs, and OPAHs in PM
92 may show significant difference between urban and background areas. For example, urban areas
93 in China with greater population, dense traffic, and developed industry emit large amount of
94 pollutants and frequently exhibit haze episodes (Wang et al., 2011b), which leads to high levels
95 of PAHs, NPAHs, and OPAHs. Conversely, background areas are typically characterized by
96 sparse population and less emission sources, and may be significantly impacted by

97 long-distance transport, where the PAHs, NPAHs and OPAHs may be relatively aged. The
98 majority of previous studies on PAHs, NPAHs, and OPAHs were conducted in urban areas, such
99 as Beijing (Wu et al., 2014), Shenyang (Miller-Schulze et al., 2010), Xi'an (Wei et al., 2015),
100 Guangzhou (Tan et al., 2011), Southern European cities (Alves et al., 2017) and Braga, Portugal
101 (Alves et al., 2016), where PAHs, NPAHs, and OPAHs are present in high concentrations.
102 Limited information has been reported on the sources and properties of PAHs, NPAHs, and
103 OPAHs in background areas in China (Liu et al., 2013) and other developing countries (Lee et
104 al., 2006), which inhibits the characterization and evaluation of regional pollution, transport,
105 and human exposure risk.

106 With the rapid economic development, China has the largest emissions of PAHs in the
107 world (annual emission 106 Gg in 2007, accounting for 21% of the global total emission) (Shen
108 et al., 2013), the North of China as one of the most polluted areas have more intensive emission
109 (Xu et al., 2005). In order to investigate the diurnal and spatial variations, sources, secondary
110 formation, long-distance transport, and cancer risk assessments of PAHs, NPAHs, and OPAHs,
111 PM_{2.5} samples were collected in three distinct locations (an urban, a mountain, and a marine site)
112 in the North of China at 3.5 h and 11.5 h intervals during the daytime and nighttime,
113 respectively.

114

115 **2. Methodology**

116

117 **2.1. Study sites and sampling**

118

119 PM_{2.5} samples were collected at three sites in the North of China. Jinan (JN), the highly
120 populated capital of Shandong Province, was selected to represent an urban environment. The
121 area is characterized by poor atmospheric diffusion conditions due to the surrounding

122 mountains on three sides and high pollutant emissions (Yang et al., 2007). The sampling site in
123 JN (36°40'N, 117°03'E; 50 m above sea level; a.s.l.) (Fig. 1) was on the rooftop of a building at
124 the central campus of Shandong University. It is surrounding by school, residential, and
125 commercial areas, with no significant stationary pollution sources. The mountain site was at the
126 summit of Mount Tai (MT, 36°15'N, 117°06'E 1465 m a.s.l.) in the southeast of Shandong
127 Province in the center of Northern China, which represents the mountain background site. It is
128 strongly influenced by the East Asian monsoon circulation and is an ideal location for
129 investigating atmospheric chemistry processing of air pollutants because the measurement site
130 was located above the nighttime planetary boundary layer. The sampling site for MT was
131 located at the Kongjun Hotel, which is far from the frequently visited zones. So the data
132 obtained in the area can be regional representative due to unique geographical location, climatic
133 conditions and negligible anthropogenic emissions. The marine sampling site Tuoji Island (TJ;
134 38°11'N, 120°44'E; 153 m a.s.l.) was located in the middle of the Bohai Strait at the distance of
135 about 40 km and 70 km from Penglai and Dalian, which is considered as the marine background
136 site. This site had the lowest elevation among the background monitoring stations and is the
137 sole marine atmospheric background station in Northern China. It is an ideal receptor site for
138 investigating continental outflow pollution. Details of the site has been described in greater
139 detail previously (Zhang et al., 2014; Zhang et al., 2016; Zhang et al., 2018).

140 $PM_{2.5}$ samples were collected in TJ from June 12 to 17, in JN from June 22 to July 04, and
141 in MT from July 09 to 23, 2015 by a mid-volume suspended particle sampler (Model TH-150 A;
142 Wuhan Tianhong Corporation, China). Quartz filters with 1 μ m pore size and 88 mm diameter
143 were used to collect samples (Pall Gelman Inc., USA,). Each filter was baked for 6 h at 600°C

144 before sampling. The flow rate of the samplers was 100 L min^{-1} , and each sampler was
145 calibrated before and after sampling. The sampling time periods per day was 7:00-10:30
146 (morning), 11:00-14:30 (day), 15:00-18:30 (evening), and 19:00-6:30 the next day (night) local
147 time. The concentration during daytime period means the average concentration during morning,
148 day and evening periods. Frequent rainfall events occurred during the sampling periods at the
149 mountain and urban sites, so 20 samples (5 samples from the four sampling time periods) were
150 selected for each site. Rainy sampling days were excluded from the analysis.

151

152 **2.2. Sample analysis**

153

154 Due to short sampling time and low levels of NPAHs and OPAHs at the background sites,
155 the sample filters (three circles with a diameter of 25 mm from every sample filter) obtained in
156 the same time interval at the same sampling site were combined prior to analysis. The combined
157 samples were analyzed by Soxhlet extraction with 150 mL dichloromethane (DCM) for 8 h. The
158 extracted samples were concentrated to about 1 mL by rotary evaporation and then fractionated
159 by silica/alumina gel columns (1 cm internal diameter \times 35 cm length). 12 cm alumina (bottom),
160 12 cm silica (middle), and 1cm anhydrous sodium sulfate (top). The silica and alumina were
161 baked for 6 h at $400 \text{ }^\circ\text{C}$ by muffle furnace and then activated at $130 \text{ }^\circ\text{C}$ for 16 h before use. The
162 purification columns were eluted by 20 mL hexane (discarded) and then by 70 mL mixture of
163 hexane and DCM (1:1, v/v) (collected). The elutes were concentrated by a rotary evaporator to
164 about 1 mL at $30 \pm 1 \text{ }^\circ\text{C}$ (water bath), added to 10 mL hexane for solvent displacement, and then
165 evaporated again to 1-2 mL by rotary evaporation. The concentrated elutes were further
166 concentrated to 1 mL under high purity nitrogen stream at $30 \pm 1 \text{ }^\circ\text{C}$. Internal standards

167 (naphthalene-d₈, anthracene-d₁₀, pyrene-d₁₀, perylene-d₁₂, 1-nitronaphthalene-d₇,
168 9-nitroanthracene-d₉, 1-nitropyrene-d₉, 6-nitrochrysene-d₁₁ and anthraquinone-d₈) were spiked
169 prior to the sample injection into the gas chromatography - mass spectrometer (GC-MS). All
170 used glassware devices were soaked in potassium dichromate lotion, rinsed by purified water
171 and ultrapure water, and then baked at 100 °C until dry.

172 A gas chromatograph coupled (GC, Agilent 7890A) with a triple quadrupole mass
173 spectrometer (MS/MS, Agilent 7000) with a 5% phenyl substituted methylpolysiloxane GC
174 column (HP-5MS, length: 30 m, diameter: 0.25 mm, film thickness: 0.25 µm, Agilent, USA)
175 was used to analyze PAHs. The system was set to use electron impact ionization (EI) in selected
176 ion monitoring (SIM) mode. The oven temperature program was held at 60°C for 1 min,
177 gradually increased to 150 °C at the rate of 40 °C/min where it was held for 5min, and then
178 increased to 300 °C at 4°C/min and held for 15min. 17 different PAHs were detected based on
179 retention time and qualitative and quantitative ions of standard PAHs. The NPAHs and OPAHs
180 was also measured by GC-MS/MS with HP-5MS column using negative chemical ionization
181 (NCI) in SIM mode. The GC oven temperature program for NPAHs and OPAHs was 60 °C for
182 1 min, ramped at 15 °C /min to 150 °C, to 300 °C at a rate of 5 °C, then held for 15 min.

183 The targeted analytes included acenaphthene (ACE), acenaphthylene (ACY), fluorene
184 (FLU), phenanthrene (PHE), anthracene (ANT), fluoranthene (FLT), pyrene (PYR),
185 benzo(a)anthracene (BaA), chrysene (CHY), benzo(b)fluoranthene (BbF), benzo(k)fluoranthene
186 (BkF), benzo(a)pyrene (BaP), benzo(e)pyrene (BeP), indeno(1,2,3-cd)pyrene (IcdP),
187 dibenzo(a,h)anthracene (DahA), benzo(g,h,i)perylene (BghiP), coronene (COR),
188 5-nitroacenaphthene (5N-ACE), 2-nitrofluorene (2N-FLU), 9-nitroanthracene (9N-ANT),

189 9-nitrophenanthrene (9N-PHE), 3-nitrophenanthrene (3N-PHE), 2-nitroanthracene (2N-ANT),
190 2+3-nitrofluoranthene (2+3N-FLT), 1-nitropyrene (1N-PYR), 2-nitropyrene (2N-PYR),
191 7-nitrobenzanthracene (7N-BaA), 6-nitrochrysene (6N-CHR), 6-nitrobenz(a)pyrene (6N-BaP),
192 9-fluorenone (9FO), anthraquinone (ATQ), phenanthrene-9-aldehyde (PHE-9-ALD),
193 benzanthrone (BZO), benzaanthracene-7,12-dione (BaAQ).

194

195 **2.3. Quality control and data analysis**

196

197 The air sampler without a denuder for reactive gaseous species removal may result in
198 sampling artifacts due to the degradation of PAHs and their derivatives (Menichini, 2009; Liu et
199 al., 2014), but the denuder-based sampling system has not yet been used widely in literature. So
200 the sampling artifacts was not considered too much in the paper, which may lead to
201 underestimation of PAHs and their derivatives, especially BaP.

202 Prior to sample analysis, surrogate standards, including acenaphthene-d₁₀, chrysene-d₁₂,
203 2-nitrofluorene-d₉ and 3-nitrofluoranthene-d₉, were spiked in 50% randomly loaded filters in
204 order to monitor the complete analysis process. The recoveries were: acenaphthene-d₁₀ 84±14%,
205 chrysene-d₁₂: 91±10%, 2-nitrofluorene-d₉: 98±26%, and 3-nitrofluoranthene-d₉: 84±15%. The
206 method recoveries were tested by spiking 50 ng, 100 ng, and 200 ng standards of target PAHs,
207 NPAHs, and OPAHs in the cleaned filters, and the recoveries were 97±15% for PAHs and
208 90±14% for derivatives. Procedural, lab, and field blanks were analyzed, and the measured
209 values of PAHs, NPAHs, and OPAHs were negligible. The blank values and recoveries were not
210 used to correct the measured values of the samples. Duplicate samples from the same filters,
211 which were extracted and measured by GC-MS/MS using the same protocol above mentioned,

212 were analyzed, and the average variation was 11.2%.

213

214 **3. Results and discussion**

215

216 **3.1. Diurnal variation of PAHs, NPAHs, and OPAHs concentrations**

217

218 The concentrations of the individual PAHs, NPAHs, and OPAHs during the four sampling
219 periods are presented in [Fig. 2](#) and [TableS. 1](#). The concentration of total PAHs at the urban site
220 ranged from 12.17 to 26.65 ng m⁻³, with a mean of 19.45 ng m⁻³, which is much higher than
221 those at the marine (between 3.07 and 6.36 ng m⁻³, with a mean value of 4.44 ng m⁻³) and
222 mountain sites (ranged from 3.27 to 6.98 ng m⁻³, with an average of 5.39 ng m⁻³). A similar
223 diurnal pattern was observed at the marine and urban site with the highest PAHs concentrations
224 during the morning and night sampling periods. This is different from the result that no
225 obviously diurnal pattern for PAHs at Mediterranean marine background site, Finokalia, Island
226 of Crete was found in [Tsapakis and Stephanou, \(2007\)](#). Direct emissions from vehicular traffic
227 during the morning period, and the lower mixing layer height and heavy truck traffic
228 (yellow-labeled vehicles were not banned in the night) during the night period likely
229 contributed to the high PAHs concentrations observed during these times. The concentration is
230 lower during the evening period likely due to the enhanced photochemical activity during the
231 day period. Most individual components showed a similar diurnal pattern at JN and TJ sites, for
232 example FLU, PHE, BaA, CHY, BbF, BkF, BaP, IcdP and BghiP, which all shows a substantial
233 morning and night rush time peak, which is slightly different from the study in PM₁₀ in
234 Birmingham UK ([Alam et al., 2015](#)) with maximum level during morning period (7:00-11:00),
235 and is similar to that in East of France at three urban sites (Strasbourg, Besancon and Spicheren)

236 in PM₁₀ with highest concentrations during morning (04:00-10:00) and evening (16:00-22:00)
237 times (Delhomme and Millet, 2012). Han et al., (2011) suggested that the peak of PAHs
238 concentration in five US counties (Maricopa, AZ, Anoka, MN, Harris, TX, Pinellas, FL and
239 Jefferson, KY) occurred during morning rush hour times (6:00), and the peak was also observed
240 during nighttime in Sacramento, CA. However, the PAHs measured at the mountain site
241 exhibited higher concentrations during the morning and day periods and the lowest
242 concentrations during the night period. Every individual species showed higher concentration
243 during the daytime (the average concentration during morning, day and evening periods),
244 compared with that during the nighttime at MT. The high elevation of the sampling location
245 (about 1500 m) may have impeded the transport of air masses from ground level to the top of
246 the mountain during the night period, resulting in the lower concentration.

247 FLT, CHY, BbF, and BghiP were the dominant PAHs at the urban site, accounting for
248 43.1%-47.3% of total PAHs, in all measurements, which indicates that the major source was
249 likely coal combustion and vehicle emissions. FLU, PHE, FLT, and CHY were dominate in the
250 samples from the marine and mountain sites, accounting for 50.9%-61.5% and 53.3%-61.0%,
251 respectively. The distinctions in the composition profiles at the urban and background sites were
252 likely due to the difference in their emission sources, photochemical degradation rates, and loss
253 due to condensation and deposition during transport (Wang et al., 2009). PAHs with molecular
254 weights between 252-300 (from BbF to COR) accounted for 33.8%-53.4% of the total PAHs
255 with higher percentages found during morning and night periods at the urban site. This was well
256 correlated with the early and late peaks in traffic emissions. Differently, the contribution of high
257 molecular weights (e.g., 5,6,7- ring PAHs) to the total PAHs was significantly lower at the

258 marine (21.3%-30.7%) and mountain (25.2%-32.7%) sites, which may be attributed to losses
259 during transport and a limited number of motor vehicles at the two sites. Previous studies have
260 also reported that high molecular weight PAHs made a large contribution to the total PAHs in
261 Xi'an, an urban site (Okuda et al., 2010) and in Malaysia, a semi-urban area (Khan et al., 2015).

262 The concentration of 12 NPAHs at the urban site ranged from 71.41 to 237.6 pg m^{-3} , with a
263 mean value of 153.7 pg m^{-3} . This was 3.61 and 3.27 times higher than in samples from the
264 marine (30.78 - 62.31 pg m^{-3} , average: 42.60 pg m^{-3}) and mountain (32.50 - 68.07 pg m^{-3} ,
265 average: 47.00 pg m^{-3}) sites. The total concentration of 12 NPAHs is almost two orders of
266 magnitude lower than the total average concentration of the 17 PAHs measured at the three sites.
267 The three most abundant NPAHs at the urban site were 9N-ANT, 2+3N-FLT, and 2N-PYR,
268 accounting for 78.2%-88.1% of total NPAHs. Similar molecular composition patterns were
269 found at the background sites, accounting for 81.5%-92.9% at the marine site and 81.2%-91.5%
270 at the mountain site. The concentrations of total NPAHs at the marine sites were higher during
271 the morning and night periods compared with those during day and evening periods, which was
272 the same as the observed diurnal variation of PAHs. However, the concentration of NPAH
273 varied considerably at the mountain site, with lowest values observed during the night period
274 and highest during the day period. This was dissimilar to the diurnal cycle of total PAHs.

275 1N-PYR, which solely originates from direct emissions (mainly from diesel powered
276 engines) (Nielsen, 1984), ranged from 5.09 to 2.22 pg m^{-3} at the urban site, with the greatest
277 concentrations occurring during periods of increased traffic. 7N-BaA exhibited similar diurnal
278 variation as 1N-PYR at the urban site, which is the most abundant compound in diesel fuel
279 particles (Finlayson-Pitts and Pitts, 2000). The concentrations of 7N-BaA were found to be the

280 highest at the urban sites, followed by the mountain site (from 0.76 to 1.81 pg m^{-3}), and then the
281 marine site (from 1.03 to 1.12 pg m^{-3}). This suggests that local emissions were relatively small
282 contributors at the background sites. The average concentration of 2+3N-FLT in the daytime
283 including morning, day and evening time periods at MT site was much higher than that in the
284 nighttime, but the same level was shown during daytime and nighttime at TJ site, and slightly
285 lower level was found in the daytime at JN than that in nighttime. But 2N-PYR had a peak
286 during morning time and was much higher in the daytime compared with that in the nighttime at
287 the three sites. This is may associated with the daytime formation of 2+3N-FLT and 2N-PYR or
288 3N-FLT from vehicle emissions possibly had a unexpected role, and the influence of NO_3 is
289 also can't be ignored. [Alam et al., \(2015\)](#) and [Tsapakis and Stephanou, \(2007\)](#) found that the
290 concentrations of 2+3N-FLT and 2N-PYR were higher in daytime than those in nighttime in
291 UK and Mediterranean.

292 The concentration of the 6 measured OPAHs was higher at the urban site (an average value
293 of 0.85 ng m^{-3}) than at the mountain (0.28 ng m^{-3}) and at the marine site (0.22 ng m^{-3}). This is
294 almost one order of magnitude lower than concurrent concentration of total PAHs. Our
295 measured OPAHs at the urban site were more concentrated than measurements conducted in
296 than Taiyuan (0.71 ng m^{-3}), Dezhou (0.03 ng m^{-3}), and Yantai (0.08 ng m^{-3}) ([Li et al., 2015](#)). The
297 concentrations of OPAHs was highest in the morning and day periods at all three sites, which is
298 distinct from the diurnal variations of PAHs and NPAHs. This difference may be partly due to
299 the fact that OPAHs are mainly emitted from solid fuel burning such as coal, firewood, and crop
300 residues in Northern China and vehicle emissions contributed relatively little to OPAHs
301 compared with to PAHs and NPAHs ([Li et al., 2015](#)). no obviously diurnal pattern of OPAHs

302 was found at Finokalia, Island of Crete without local emissions (Tsapakis and Stephanou, 2007).
303 The six OPAHs components all presented higher levels in the daytime than those in the
304 nighttime in marine and mountain background sites. The most abundant OPAH was 9FO,
305 followed by ATQ in the three sites, accounting for 80.9%- 96.1% of total OPAHs.

306
307
308

3.2. Source diagnostics

309 Diagnostic ratios are frequently used to identify the sources of PAHs because the
310 distributions of the homologues are strongly related with the formation mechanisms of organic
311 species with similar characteristics (Kavouras, 2001). Diagnostic tool should be used with
312 caution because some ratios are variable in the atmosphere due to the different degradation
313 ratios of some PAH species (Ding et al., 2007).

314 FLT, PYR, IcdP and BghiP have comparable degradation ratios (Behymer and Hites, 1988),
315 so the ratios of $FLT/(FLT+PYR)$ and $IcdP/(IcdP+BghiP)$ can reveal original compositional
316 information during transportation and ensure the accuracy of source evaluation at receptor sites.
317 A $FLT/(FLT+PYR)$ ratio higher than 0.5 indicates coal/biomass burning and between 0.4 and
318 0.5 indicates petroleum combustion (Pio et al., 2001; Yunker et al., 2002), as shown in Table 1.
319 A ratio of $IcdP/(IcdP+BghiP)$ higher than 0.5 indicates coal/ biomass combustion, and a ratio
320 lower than 0.2 is characteristic of petroleum source. A $IcdP/(IcdP+BghiP)$ ratio between 0.2 and
321 0.5 (or 0.18-0.40) indicates petroleum combustion (Pio et al., 2001; Yunker et al., 2002). The
322 $IcdP/(IcdP+BghiP)$ ratios ranged from 0.40 to 0.43, with an average value of 0.41 at the urban
323 site (Table 1), implying that petroleum combustion was a strong contributor. Comparable values
324 were also observed in other Chinese cities, such as Shanghai (Feng et al., 2006), Beijing (Okuda
325 et al., 2006), Qingdao (Guo et al., 2003), and Nanjing (Wang et al., 2006). A negligible

326 difference in the IcdP/(IcdP+BghiP) ratio at the marine (from 0.37 to 0.42, average: 0.39),
327 mountain (from 0.42 to 0.47, average: 0.45), and urban sites was found. The ratio is lower than
328 those obtained in Florence, a urban background site and Athens, a suburban site (all higher than
329 0.5) in summer (Alves et al., 2017). But the ratios of IcdP/(IcdP+BghiP) at the background sites
330 in this paper were comparable with that previously obtained at the Yellow River Delta National
331 Nature Reserve (YRDNNR) in the summer (0.46) (Zhu et al., 2014). The average values of the
332 FLT/(FLT+PYR) ratio at the urban (0.68), marine (0.68), and mountain (0.66) sites were similar,
333 and all were higher than 0.5 indicating that coal or biomass combustion was a main source. The
334 ratios were slightly higher than those at Florence and Athens (all higher than 0.5, but lower than
335 0.6) in summer, but much higher than that in Oporto, a urban site (lower than 0.3) (Alves et al.,
336 2017). No obvious diurnal variations of the ratios were observed at the three sites, indicating
337 that the main source did not change during different sampling intervals. In conclusion, the two
338 diagnostic ratios suggest that fossil fuel and biomass combustion were the main sources at the
339 urban and background sites during the summer.

340 BaA and BaP degrade faster than their corresponding homologues (CHR and BeP), which
341 may significantly influence diagnostic ratios for source and downwind regions (Behymer and
342 Hites, 1988; Zhang et al., 2005). By leveraging these isomer pairs (BaA/CHR and BaP/BeP) the
343 residence time of particulate PAHs in the atmosphere can be evaluated. The ratios of BaP/BeP
344 and BaA/CHR were plotted in Fig. 3A and 3B during the four sampling periods for the urban,
345 marine, and mountain sites. The average ratios were the highest at the urban site (BaA/CHR:
346 0.46 and BaP/BeP: 0.46), and the lowest ratios were observed at the marine site ((BaA/CHR:
347 0.34 and BaP/BeP: 0.27), implying that the air masses collected at the urban site were relatively

348 fresh and most aged at the marine site. The ratios at the marine and mountain sites during the
349 sampling periods were persistently less than 0.4, suggesting that air masses were strongly
350 influenced by photo-degradation and long distance transport likely played an important role
351 (Liu et al., 2013). In the urban area, the ratios of BaA/CHR and BaP/BeP were relatively low in
352 day and evening periods, indicating the influence of photochemical reaction. The diurnal
353 patterns of BaP/BeP in marine area was the same with that in urban area, but was different from
354 that in mountain areas with higher values in day and night periods.

355 The ratio of 2N-FLT/1N-PYR has been traditionally applied to differentiate primary
356 emission and secondary formation of NPAHs in the atmosphere. 1N-PYR mainly derived from
357 diesel powered engines (Nielsen, 1984), while 2N-FLT is known to be formed by atmospheric
358 photochemical reactions initiated by OH radicals in the daytime and NO₃ radicals in the
359 nighttime, and has never been observed from direct emissions (Arey et al., 1986). A ratio of
360 2N-FLT/1N-PYR higher than 5 indicates secondary formation of NPAHs, while a ratio lower
361 than 5 indicates the primary emissions (Albinet et al., 2007; Bandowe et al., 2014). In our study,
362 the isomers of 2N-FLT and 3N-FLT were not separated by our GC-column HP-5MS and
363 analytical procedure. However, many previous studies have reported that 2+3N-FLT/1N-PYR
364 can be used in lieu of to replace the original 2N-FLT/1N-PYR ratio due to negligible abundant
365 of 3N-FLT in the air compared with 2N-FLT (Bamford and Baker, 2003). Fig.3C presents the
366 ratios of 2+3N-FLT/1N-PYR from the three sites during the four sampling periods. While the
367 average value at the urban site (17.5) was significant lower than that at the marine (27.3) and
368 mountain (25.8) sites, this diagnostic ratio reveals that atmospheric secondary formation of
369 2N-FLT dominated at the urban and background sites. The ratio values were comparable to that

370 obtained in the North China in the hot season (23.6) (Lin et al., 2015), but much lower than that
371 (89.1) observed during the winter in Wanqingsha, the South of China (Huang et al., 2014). The
372 greatest ratio (24.9) at the urban site was found in the day samples during periods of highest
373 photochemical activity, which is similar to that at the mountain site. The ratio at the marine site
374 was the highest in the morning period.

375 The ratio of 2N-FLT/2N-PYR has been widely used to explore the occurrence and relative
376 importance of OH vs NO₃ radical initiated oxidation pathways for the formation of NPAHs in
377 the atmosphere (Arey et al., 1986). 2N-PYR is formed from PYR reacting with an OH radical in
378 the presence of NO₂, but is not formed from the reaction with NO₃ radical (Arey et al., 1986). A
379 ratio close to 10 indicates the dominance of the OH radical-initiated reaction, while a ratio close
380 to 100 indicates that the NO₃ radical-initiated reactions dominate NPAHs formation (Albinet et
381 al., 2007; Wang et al., 2011a). In our study, the average ratios at the urban (4.0), marine (9.6),
382 and mountain sites (8.8) (Fig.3D) were all less than 10, indicating the domination of day-time
383 OH radical-initiated formation pathways. This is consistent with previously reported values
384 from the summer season in North China (4.5) (Lin et al., 2015) and in Beijing (below 10)
385 (Wang et al., 2011a). The highest ratios were observed during the night period at the urban site,
386 which is similar to trends at the two background sites. The ratios at the background sites were
387 significantly higher than the urban site, which may partly be due to the higher concentration of
388 NO in the urban atmosphere because the reaction of NO₃ with NO leads to low level of NO₃
389 (Huang et al., 2014).

390

391 **3.3.Evaluation of excess cancer risk**

392

393 The lifetime excess cancer risk from inhalation (ECR) of PAH and NPAHs mixtures was
394 applied to assess the carcinogenicity of the samples. This method has been recommended by the
395 Office of Environmental Health Hazard Assessment (OEHHA) of the California Environmental
396 Protection Agency (CalEPA) and has been widely utilized in many previous studies (Bandowe
397 et al., 2014; Wei et al., 2015; Zhu et al., 2014; Ramirez et al., 2011; Alves et al., 2017). The
398 carcinogenic risk of each PAH or NPAH compound was estimated based on its BaP equivalent
399 concentration (BaP_{eqi}), which is calculated by multiplying individual compound concentration
400 ($C_i \text{ ng m}^{-3}$) by the corresponding toxicity equivalency factor (TEF_i) as Eq (1). The TEF values
401 for 15 PAHs and 6 NPAHs were taken from Collins et al., (1998) and Nisbet and Lagoy (1992),
402 who reported the toxic potency of each PAH or NPAH relative to BaP (Petry et al., 1996). The
403 risk of OPAHs was not evaluated due to the lack of available TEF data. Using Eq (1), the toxic
404 equivalency (TEQ) is the sum of target compound BaP_{eq} .

$$405 \quad BaP_{eqi} = C_i * TEF_i \quad \text{and} \quad TEQ = \sum(C_i * TEF_i) \quad (1)$$

406 ECR was assessed by employing Eq (2), where UR_{BaP} is the unit inhalation cancer risk
407 factor of BaP. The UR_{BaP} is defined as the number of people who will develop cancer from the
408 inhalation of 1 ng/m^3 BaP_{eq} within a lifetime of 70 years. The UR_{BaP} was suggested to be $8.7 \times$
409 $10^{-5} (\text{ng m}^{-3})^{-1}$ by the World Health Organization (WHO) and $1.1 \times 10^{-6} (\text{ng m}^{-3})^{-1}$ by CalEPA
410 (OEHHA, 1994; WHO, 2000). This means that 8.7 or 0.11 cases per 100,000 people with
411 inhalational exposure to 1 ng/m^3 of BaP over a lifetime of 70 years would have cancer risk.

$$412 \quad ECR = TEQ * UR_{BaP} \quad (2)$$

413 The mean TEQ at the urban site was 2.49 ng m^{-3} for the 21 target compounds, which is
414 substantially higher than for the mountain (0.43 ng m^{-3}) and marine (0.33 ng m^{-3}) sites. The

415 TEQ at the urban site was much lower than the national standard of 10 ng m^{-3} , but higher than
416 the WHO standard (1 ng m^{-3}) (Ventafriidda et al., 1987). The value at the urban location was
417 also much lower than what was previously calculated for Beijing, China (Jia et al., 2011), Xi'an,
418 China (Bandowe et al., 2014) and Zonguldak, Turkey (Akyuz and Cabuk, 2008), but higher than
419 those for western and southern European cities (Martellini et al., 2012; Alves et al., 2017). The
420 values at the marine and mountain locations were comparable with that observed in the
421 YRDNNR in summer (0.45 ng m^{-3}) (Zhu et al., 2014). BbF, BaP, IcdP, and DahA, especially
422 DahA and BaP, contributed significantly to the TEQ value at the three sites. The actual TEQ
423 may be higher in view of the BaP degradation by O_3 during air sampling on the filters
424 (Menichini et al., 2009). The TEQ diurnal patterns at the three sites were consistent with the
425 daily variation of total PAHs concentration, which was highest during morning and night
426 periods at the urban and marine sites and during morning and day periods at mountain site. The
427 contribution of average TEQ of 6 NPAHs to the total TEQ was larger at the background sites
428 (MT, 1.72% and TJ, 1.34%) than that at the urban site (0.41%), which may due to the influence
429 of secondary formation of NPAHs during long-distance transport and high concentration of
430 PAHs at urban site.

431 The average ECR for 70 years' life span was 2.17×10^{-4} (WHO method) and 2.74×10^{-6}
432 (CalEPA method) at the urban site. Hence, inhalation of the 21 measured compounds could
433 result in 217 or 3 cases of cancer per million adult residents in Jinan, respectively. This was
434 higher than estimates for the marine (29 WHO method and 1 CalEPA method cases per million)
435 and mountain (38 WHO method and 1 CalEPA method cases per million) sites. The lower ECR
436 at background sites is likely attributable to less direct source emissions, lower population, and

437 favorable diffusion conditions. The acceptable or negligible threshold of ECR using WHO
438 method based on American Environmental Protection Agency is 10^{-6} , so the lifetime excess
439 cancer risk should be paid attention for healthy protection in the future in the Chinese cities.

440

441 **4. Summary**

442

443 In this study, PAHs, NPAHs, and OPAHs were investigated during the summer in the
444 Northern China at an urban site and two background sites at 3.5 h and 11.5 h sampling intervals.
445 The average concentrations of PAHs, NPAHs, and OPAHs at the urban site were 19.45 ng m^{-3} ,
446 153.7 pg m^{-3} , and 0.85 ng m^{-3} , respectively, which were 3.61-4.38 and 3.05-3.61 times higher
447 than those at marine and mountain sites, respectively. The concentrations of PAHs and NPAHs
448 were greatest during morning and night periods at the urban and marine sites and during
449 morning and day periods at the mountain site. The concentration of OPAHs was highest during
450 the morning and day periods at all the three sites. The diurnal variations of high molecular
451 weight PAHs (e.g., 1N-PRY and 7N-BaA) at the urban site was closely linked to vehicle
452 emissions.

453 On the basis of diagnostic ratios, the main sources of PAHs were found to be fossil fuel
454 and biomass combustion. The air masses at the background sites, especially at the marine site,
455 were more aged compared with those at the urban site. The atmospheric reactions were most
456 efficient at the marine site, followed by the mountain site. The main reaction pathway was
457 OH-initiated radical reactions at the urban and background sites. The contribution of secondary
458 formation to the total PAHs was largest during the day period at the urban and mountain sites
459 and during morning period at the marine site.

460 The mean toxicity equivalency factor at the urban site was higher than those at marine and
461 mountain sites and greater than the guidelines suggested by the World Health Organization. The
462 average excess cancer risk from inhalation (ECR) for 70 years' life span was highest at the
463 urban site.

464

465 **Acknowledgements**

466

467 This work was supported by the National Natural Science Foundation of China (Nos.
468 21577079 and 21307074). This project has received funding from the European Union's
469 Horizon 2020 research and innovation programme under grant agreement No 690958.

470

471 **References**

472

473 Abdel-Shafy, H., Mansour, M., 2016. A review on polycyclic aromatic hydrocarbons: Source,
474 environmental impact, effect on human health and remediation. Egyptian Journal of
475 Petroleum 25, 107-123.

476 Akyüz, M., Çabuk, H., 2008. Particle-associated polycyclic aromatic hydrocarbons in the
477 atmospheric environment of Zonguldak, Turkey. Sci. Total Environ. 405, 62-70.

478 Alam, M., Keyte, I., Yin, J., Stark, C., Jones, A., Harrison, R., 2015. Diurnal variability of
479 polycyclic aromatic compound (PAC) concentrations: Relationship with meteorological
480 conditions and inferred sources. Atmos. Environ. 122, 427-438.

481 Albinet, A., Leoz-Garziandia, E., Budzinski, H., Viilenave, E., 2007. Polycyclic aromatic
482 hydrocarbons (PAHs), nitrated PAHs and oxygenated PAHs in ambient air of the

483 Marseilles area (South of France): concentrations and sources. *Sci. Total Environ.* 384,
484 280-292.

485 Albinet, A., Leoz-Garziandia, E., Budzinski, H., Villenave, E., Jaffrezo, J.L., 2008. Nitrated and
486 oxygenated derivatives of polycyclic aromatic hydrocarbons in the ambient air of two
487 French alpine valleys Part 1: Concentrations, sources and gas/particle partitioning. *Atmos.*
488 *Environ.* 42, 43-54.

489 Alves, C., Vicente, A., Gomes, J., Nunes, T., Duarte, M., Bandowe, B., 2016. Polycyclic aromatic
490 hydrocarbons (PAHs) and their derivatives (oxygenated-PAHs, nitrated-PAHs and
491 azaarenes) in size-fractionated particles emitted in an urban road tunnel. *Atmos. Res.* 180,
492 128-137.

493 Alves, C., Vicente, A., Custódio, D., Cerqueira, M., Nunes, T., Pio, C., Lucarelli, F., Calzolari, G.,
494 Nava, S., Diapouli, E., Eleftheriadis, K., Querol, X., Bandowe, B., 2017. Polycyclic
495 aromatic hydrocarbons and their derivatives (nitro-PAHs, oxygenated PAHs, and
496 azaarenes) in PM_{2.5} from Southern European cities. *Sci. Total Environ.* 595, 494-504

497 Arey, J., Zielinska, B., Atkinson, R., Winer, A.M., Ramdahl, T., Pitts, J.N., 1986. The formation of
498 nitro-PAH from the gas-phase reactions of fluoranthene and pyrene with the OH radical
499 in the presence of NO_x. *Atmos. Environ.* 20, 2339–2345.

500 Balducci, C., Cecinato, A., Paolini, V., Guerriero, E., Perilli, M., Romagnoli, P., Tortorella, C.,
501 Iacobellis, S., Giove, A., Febo, A., 2018. Volatilization and oxidative artifacts of PM
502 bound PAHs collected at low volume sampling (1): Laboratory and field evaluation.
503 *Chemosphere.* 200, 106-115.

504 Bamford, H., Baker, J., 2003. Nitro-polycyclic aromatic hydrocarbon concentrations and sources

505 in urban and suburban atmospheres of the mid-Atlantic region. *Atmos. Environ.* 37,
506 2077–2091.

507 Bandowe, B., Meusel, H., Huang, R., Ho, K., Cao, J., Hoffmann, T., 2014. PM_{2.5}-bound
508 oxygenated PAHs, nitro-PAHs and parent-PAHs from the atmosphere of a Chinese
509 megacity: seasonal variation, sources and cancer risk assessment. *Sci. Total Environ.*
510 473-474, 77-87.

511 Behymer, T., Hites, R., 1988. Photolysis of polycyclic aromatic hydrocarbons adsorbed on fly ash.
512 *Environ. Sci. Technol.* 22, 1311–1319.

513 Collins, J., Brown, J., Alexeeff, G., Salmon, A., 1988. Potency equivalency factors for some
514 polycyclic aromatic hydrocarbons and polycyclic aromatic hydrocarbon derivatives.
515 *Regul Toxicol Pharmacol* 28, 45–54.

516 Delhomme, O., Millet, M., 2012. Characterization of particulate polycyclic aromatic hydrocarbons
517 in the east of France urban areas. *Environ. Sci. Pollut. Res.* 19, 1791-17.

518 Ding, X., Wang, X., Xie, Z., Xiang, C., Mai, B., Sun, L., 2007. Atmospheric polycyclic aromatic
519 hydrocarbons observed over the North Pacific Ocean and the Arctic area: Spatial
520 distribution and source identification. *Atmos. Environ.* 41, 2061-2072.

521 Elorduy, I., Elcoroaristizabal, S., Durana, N., García, J.A., Alonso, L., 2016. Diurnal variation of
522 particle-bound PAHs in an urban area of Spain using TD-GC/MS: Influence of
523 meteorological parameters and emission sources. *Atmos. Environ.* 138, 87-98.

524 Feng, J., Chan, C.K., Fang, M., Hu, M., He, L., Tang, X., 2006. Characteristics of organic matter
525 in PM_{2.5} in Shanghai. *Chemosphere* 64, 1393-400.

526 Finlayson-Pitts, B.J., Pitts J.N., 2000. *Chemistry of the Upper and Lower Atmosphere*. Academic

527 Press, San Diego.

528 Guo, Z.G., Sheng, L.F., Feng, J.L., Fang, M., 2003. Seasonal variation of solvent extractable
529 organic compounds in the aerosols in Qingdao, China. *Atmos. Environ.* 37, 1825-1834.

530 Han, I., Ramos-Bonilla, J., Rule, A., Mihalic, J., Polyak, L., Breysse, P., Geyh, A., 2011
531 Comparison of spatial and temporal variations in p-PAH, BC, and p-PAH/BC ratio in six
532 US counties. *Atmos. Environ.* 45, 7644-7652.

533 Huang, B., Liu, M., Bi, X., Chaemfa, C., Ren, Z., Wang, X., 2014. Phase distribution, sources and
534 risk assessment of PAHs, NPAHs and OPAHs in a rural site of Pearl River Delta region,
535 China. *Atmos. Pollut. Res.* 5, 210-218.

536 Jariyasopit, N., Zimmermann, K., Schrlau, J., Arey, J., Atkinson, R., Yu, T.W., 2014.
537 Heterogeneous reactions of particulate matter-bound PAHs and NPAHs with NO₃/N₂O₅,
538 OH radicals, and O₃ under simulated long-range atmospheric transport conditions:
539 reactivity and mutagenicity. *Environ. Sci. Technol.* 48, 10155-10164.

540 Jia, Y., Stone, D., Wang, W., Schrlau, J., Tao, S., Simonich, S.L.M., 2011. Estimated reduction in
541 cancer risk due to PAH exposures if source control measures during the 2008 Beijing
542 Olympics were sustained. *Environ. Health Perspect.* 119, 815–820.

543 Kavouras, I.G., Koutrakis, P., Tsapakis, M., Lagoudaki, E., Stephanou, E.G., Baer, D.V., Oyola, P.,
544 2001. Source Apportionment of Urban Particulate Aliphatic and Polynuclear Aromatic
545 Hydrocarbons (PAHs) Using Multivariate Methods. *Environ. Sci. Technol.* 35, 2288-2294.

546 Khan, M., Latif, M., Lim, C., Amil, N., Jaafar, S., Dominick, D., 2015. Nadzir, M., Sahani, M.,
547 Tahir, N., 2015 Seasonal effect and source apportionment of polycyclic aromatic
548 hydrocarbons in PM_{2.5}. *Atmos. Environ.* 106, 178-190.

549 Kojima, Y., Inazu, K., Hisamatsu, Y., Okochi, H., Baba, T., Nagoya, T., 2010. Influence of
550 secondary formation on atmospheric occurrences of oxygenated polycyclic aromatic
551 hydrocarbons in airborne particles. *Atmos. Environ.* 44, 2873-2880.

552 Lee, J.Y., Kim, Y.P., Kang, C.H., Ghim, Y.S., 2006. Seasonal trend of particulate PAHs at Gosan, a
553 background site in Korea between 2001 and 2002 and major factors affecting their levels.
554 *Atmos. Res.* 82, 680-687.

555 Li, W., Wang, C., Shen, H., Su, S., Shen, G., Huang, Y., 2015. Concentrations and origins of
556 nitro-polycyclic aromatic hydrocarbons and oxy-polycyclic aromatic hydrocarbons in
557 ambient air in urban and rural areas in northern China. *Environ. Pollut.* 197, 156-164.

558 Lin, Y., Qiu, X., Ma, Y., Ma, J., Zheng, M., Shao, M., 2015. Concentrations and spatial
559 distribution of polycyclic aromatic hydrocarbons (PAHs) and nitrated PAHs (NPAHs) in
560 the atmosphere of North China, and the transformation from PAHs to NPAHs. *Environ.*
561 *Pollut.* 196, 164-170.

562 Liu, J., Li, J., Lin, T., Liu, D., Xu, Y., Chaemfa, C., 2013. Diurnal and nocturnal variations of
563 PAHs in the Lhasa atmosphere, Tibetan Plateau: Implication for local sources and the
564 impact of atmospheric degradation processing. *Atmos. Res.* 124, 34-43.

565 Liu, K., Duan, F., He, K., Ma, Y., Cheng, Y., 2014. Investigation on sampling artifacts of particle
566 associated PAHs using ozone denuder systems. *Front. Environ. Sci. Eng.* 8, 284-292

567 Loomis, D., Grosse, Y., Lauby-Secretan, B., Ghissassi, F.E., Bouvard, V., Benbrahim-Tallaa, L.,
568 2013. The carcinogenicity of outdoor air pollution. *The Lancet Oncology.* 14, 1262-1263.

569 Łuczyński, M., Góra, M., Brzuzan, P., Wilamowski, J., Kozik, B., 2005. Oxidative metabolism,
570 mutagenic and carcinogenic properties of some polycyclic aromatic hydrocarbons.

571 Environmental Biotechnology 1, 16-28.

572 Martellini, T., Giannoni, M., Lepri, L., Katsoyiannis, A., Cincinelli, A., 2012. One year intensive
573 PM_{2.5}-bound polycyclic aromatic hydrocarbons monitoring in the area of Tuscany, Italy.
574 Concentrations, source understanding and implications. Environ. Pollut. 164, 252–258.

575 Menichini, E., 2009. On-filter degradation of particle-bound benzo[a]pyrene by ozone during air
576 sampling: A review of the experimental evidence of an artefact. Chemosphere. 77,
577 1275-1284.

578 Miller-Schulze, J.P., Paulsen, M., Toriba, A., Tang, N., Hayakawa, K., Tamura, K.J., Dong, L.J.,
579 Zhang, X.M., Simpson, C.D., 2010. Exposures to Particulate Air Pollution and
580 Nitro-Polycyclic Aromatic Hydrocarbons among Taxi Drivers in Shenyang, China.
581 Environ. Sci. Technol. 44, 216-221.

582 Nielsen, T., 1984. Reactivity of polycyclic aromatic hydrocarbons toward nitrating species.
583 Environ. Sci. Technol. 18, 157–163.

584 Nisbet, I.C.T., Lagoy, P.K., 1992. Toxic equivalency factors (TEFs) for polycyclic aromatic
585 hydrocarbons (PAHs). Regul Toxicol Pharmacol 16, 290–300.

586 OEHHA. 1994. Benzo[a]pyrene as a toxic air contaminant. Berkeley, California, USA: California
587 Environmental Protection Agency [[http://www.arb.ca.gov/toxics/id/summary/ bap.pdf](http://www.arb.ca.gov/toxics/id/summary/bap.pdf)
588 accessed March 19, 2013].

589 Okuda, T., Naoi, D., Tenmoku, M., Tanaka, S., He, K., Ma, Y., 2006. Polycyclic aromatic
590 hydrocarbons (PAHs) in the aerosol in Beijing, China, measured by aminopropylsilane
591 chemically-bonded stationary-phase column chromatography and HPLC/fluorescence
592 detection. Chemosphere 65, 427-435.

593 Okuda, T., Okamoto, K., Tanaka, S., Shen, Z., Han, Y., Huo, Z., 2010. Measurement and source
594 identification of polycyclic aromatic hydrocarbons (PAHs) in the aerosol in Xi'an, China,
595 by using automated column chromatography and applying positive matrix factorization
596 (PMF). *Sci. Total Environ.* 408, 1909-1914.

597 Pedersen, D.U., Durant, J.L., Taghizadeh, K., Hemond, H.F., Lafleur, A.L., Cass, G.R., 2005.
598 Human Cell Mutagens in Respirable Airborne Particles from the Northeastern United
599 States. 2. Quantification of Mutagens and Other Organic Compounds. *Environ. Sci.*
600 *Technol.* 39, 9547-9560.

601 Petry, T., Schmid, P., Schlatter, C., 1996. The use of toxic equivalency factors in assessing
602 occupational and environmental health risk associated with exposure to airborne mixtures
603 of polycyclic aromatic hydrocarbons (PAHs). *Chemosphere* 32, 639-648.

604 Pio, C.A., Alves, C.A., Duarte, A.C., 2001. Identification, abundance and origin of atmospheric
605 organic particulate matter in a Portuguese rural area. *Atmos. Environ.* 35, 1365-1375.

606 Ramírez, N., Cuadras, A., Rovira, E., Marcé, R., Borrull, F., 2011. Risk Assessment Related to
607 Atmospheric Polycyclic Aromatic Hydrocarbons in Gas and Particle Phases near
608 Industrial Sites. *Environ. Health Perspective.* 119, 1110-1116.

609 Reisen, F., Arey, J., 2005. Atmospheric reactions influence seasonal PAH and nitro-PAH
610 concentrations in the Los Angeles basin. *Environ. Sci. Technol.* 39, 64-73.

611 Ringuet, J., Albinet, A., Leoz-Garziandia, E., Budzinski, H., Villenave, E., 2012. Diurnal/nocturnal
612 concentrations and sources of particulate-bound PAHs, OPAHs and NPAHs at traffic and
613 suburban sites in the region of Paris (France). *Sci. Total Environ.* 437, 297-305.

614 Seinfeld, J.H., Carmichael, G.R., Arimoto, R., Conant, W.C., Brechtel, F.J., Bates, T.A., Cahill,

615 T.A., Clarke, A.D., Doherty, S.J., Flatau, P.J., Huebert, B.J., Kim, J., Markowicz, K.M.,
616 Quinn, P.K., Russell, L.M., Russell, P. B., Shimizu, A., Shinozuka, Y., Song, C.H., Tang,
617 Y.H., Uno, I., Vogelmann, A.M., Weber, R.J.,Woo, J.H., and Zhang, X.Y., 2004.
618 ACE-Asia: Regional climatic and atmospheric chemical effects of Asian dust and
619 pollution. *B. Am. Meteorol. Soc.* 85, 367–380.

620 Shen, H., Huang, Y., Wang, R., Zhu, D., Li, W., Shen, G., Wang, B., Zhang, Y., Chen, Y., Lu,
621 Y., Chen, H., Li, T., Sun, K., Li, B., Liu, W., Liu, J., Tao, S., 2013. Global
622 atmospheric emissions of polycyclic aromatic hydrocarbons from 1960 to 2008 and
623 future predictions. *Environ. Sci. Technol.*47, 6415-6424.

624 Souza, K., Carvalho, L., Allen, A., Cardoso, A., 2014. Diurnal and nocturnal measurements of
625 PAH, nitro-PAH, and oxy-PAH compounds in atmospheric particulate matter of a sugar
626 cane burning region. *Atmos. Environ.* 83, 193-201.

627 Tan, J., Guo, S., Ma, Y., Duan, J., Cheng, Y., He, K., 2011. Characteristics of particulate PAHs
628 during a typical haze episode in Guangzhou, China. *Atmos. Res.* 102, 91-98.

629 Tsapakis, M., Stephanou, E.G., 2007. Diurnal Cycle of PAHs, Nitro-PAHs, and oxy-PAHs in a
630 High Oxidation Capacity Marine Background Atmosphere. *Environ. Sci. Technol.* 41,
631 8011-8017.

632 Ventafridda, V., Tamburini, M., Caraceni, A., 1987. A validation study of the WHO method for
633 cancer pain relief. *Cancer* 59, 850–856.

634 Wang, G., Huang, L., Xin, Z., Niu, H., Dai, Z., 2006. Aliphatic and polycyclic aromatic
635 hydrocarbons of atmospheric aerosols in five locations of Nanjing urban area, China.
636 *Atmos. Res.* 81, 54-66.

637 Wang, G.H., Kawamura, K., Xie, M., Hu, S., Gao, S., Cao, J., An, Z., Wang, Z., 2009.
638 Size-distributions of n-alkanes, PAHs and hopanes and their sources. *Atmos. Chem. Phys.*
639 9, 8869-8882.

640 Wang, G.H., Li, J.J., Cheng, C.L., Zhou, B.H., Xie, M.J., Hu, S.Y., 2012. Observation of
641 atmospheric aerosols at Mt. Hua and Mt. Tai in central and east China during spring 2009
642 – Part 2: Impact of dust storm on organic aerosol composition and size distribution.
643 *Atmos. Chem. Phys.* 12, 4065-4080.

644 Wang, W., Jariyasopit, N., Schrlau, J., Jia, Y., Tao, S., Yu, T.W., 2011a. Concentration and
645 photochemistry of PAHs, NPAHs, and OPAHs and toxicity of PM_{2.5} during the Beijing
646 Olympic Games. *Environ. Sci. Technol.* 45, 6887-6895.

647 Wang, W., Simonich, S.L.M., Giri, B., Xue, M., Zhao, J., Chen, S., 2011b. Spatial distribution and
648 seasonal variation of atmospheric bulk deposition of polycyclic aromatic hydrocarbons in
649 Beijing-Tianjin region, North China. *Environ. Pollut.* 159, 287-293.

650 Wang, Y., Wang, M.H., Zhang, R.Y., Ghanc, S.J., Lin, Y., Hua, J.X., Pan, B., Levy, M., Jiang, J.H.,
651 Molinae, M.J., 2014. Assessing the effects of anthropogenic aerosols on Pacific storm
652 track using a multiscale global climate model. *PNAS.* 11, 6894-6899.

653 Wei, C., Han, Y., Bandowe, B.A., Cao, J., Huang, R.J., Ni, H., 2015. Occurrence, gas/particle
654 partitioning and carcinogenic risk of polycyclic aromatic hydrocarbons and their oxygen
655 and nitrogen containing derivatives in Xi'an, central China. *Sci. Total Environ.* 505,
656 814-822.

657 WHO. Air quality guidelines for Europe. Copenhagen, Denmark: WHO Regional Office for
658 Europe; 2000 [http://www.euro.who.int/__data/assets/pdf_file/0005/74732/E71922.pdf]

659 accessed March 19, 2013].

660 Wu, Y., Yang, L., Zheng, X., Zhang, S., Song, S., Li, J., 2014. Characterization and source
661 apportionment of particulate PAHs in the roadside environment in Beijing. *Sci. Total*
662 *Environ.* 470-471, 76-83.

663 Xu, S., Liu, W., Tao, S., 2005. Emission of polycyclic aromatic hydrocarbons in China. *Environ.*
664 *Sci. Technol.* 40, 702-708.

665 Yang, L.X., Wang, D.C., Cheng, S.H., Wang, Z., Zhou, Y., Zhou, X.H., 2007. Influence of
666 meteorological conditions and particulate matter on visual range impairment in Jinan,
667 China. *Sci. Total Environ.* 383, 164-173.

668 Yunker, M.B., Macdonald, R.W., Vingarzan, R., Mitchell, H.R., Goyette, D.,
669 Sylvestre, S., 2002. PAHs in the Fraser River basin: a critical appraisal PAH
670 ratios as indicators of PAH source and composition. *Organic Geochemistry* 33, 489-515.

671 Zhang, Y., Tao, S., Liu, W., Yang, Y., Zuo, Q., Liu, S., 2005. Source
672 diagnostics of polycyclicaromatic hydrocarbons based on species ratios: a
673 multimedia approach. *Environ. Sci. Technol.* 39, 9109-9114.

674 Zhang, F., Chen, Y., Tian, C., Wang, X., Huang, G., Fang, Y., 2014. Identification and
675 quantification of shipping emissions in Bohai Rim, China. *Sci. Total Environ.* 497-498,
676 570-577.

677 Zhang, J., Yang, L., Mellouki, A., Wen, L., Yang, Y., Gao, Y., 2016. Chemical characteristics and
678 influence of continental outflow on PM_{1.0}, PM_{2.5} and PM₁₀ measured at Tuoji island in the
679 Bohai Sea. *Sci. Total Environ.* 573, 699-706.

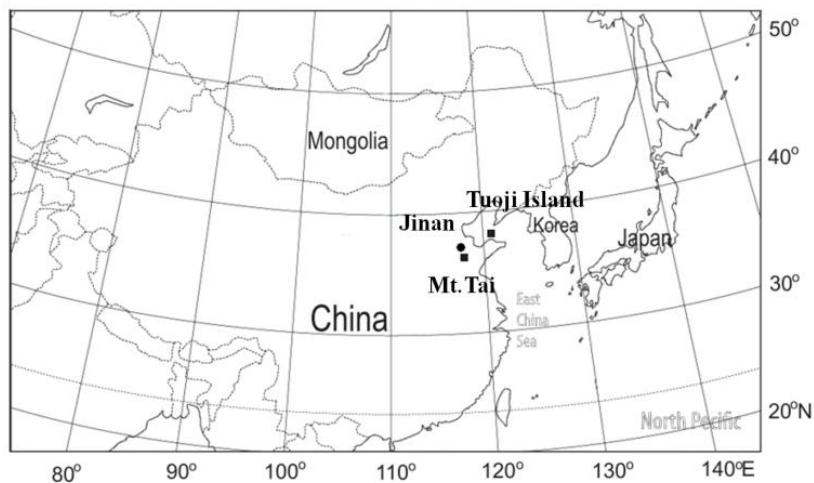
680 Zhang, J., Yang, L., Mellouki, A., Chen, J., Chen, X., Gao, Y., Jiang, P., Li, Y., Yu, H., Wang, W.,

681 2018. Atmospheric PAHs, NPAHs, and OPAHs at an urban, mountainous, and marine
682 sites in Northern China: Molecular composition, sources, and ageing. *Atmos. Environ.* 173,
683 256-264.

684 Zhu, Y., Yang, L., Yuan, Q., Yan, C., Dong, C., Meng, C., 2014. Airborne particulate polycyclic
685 aromatic hydrocarbon (PAH) pollution in a background site in the North China Plain:
686 concentration, size distribution, toxicity and sources. *Sci. Total Environ.* 466-467,
687 357-368.

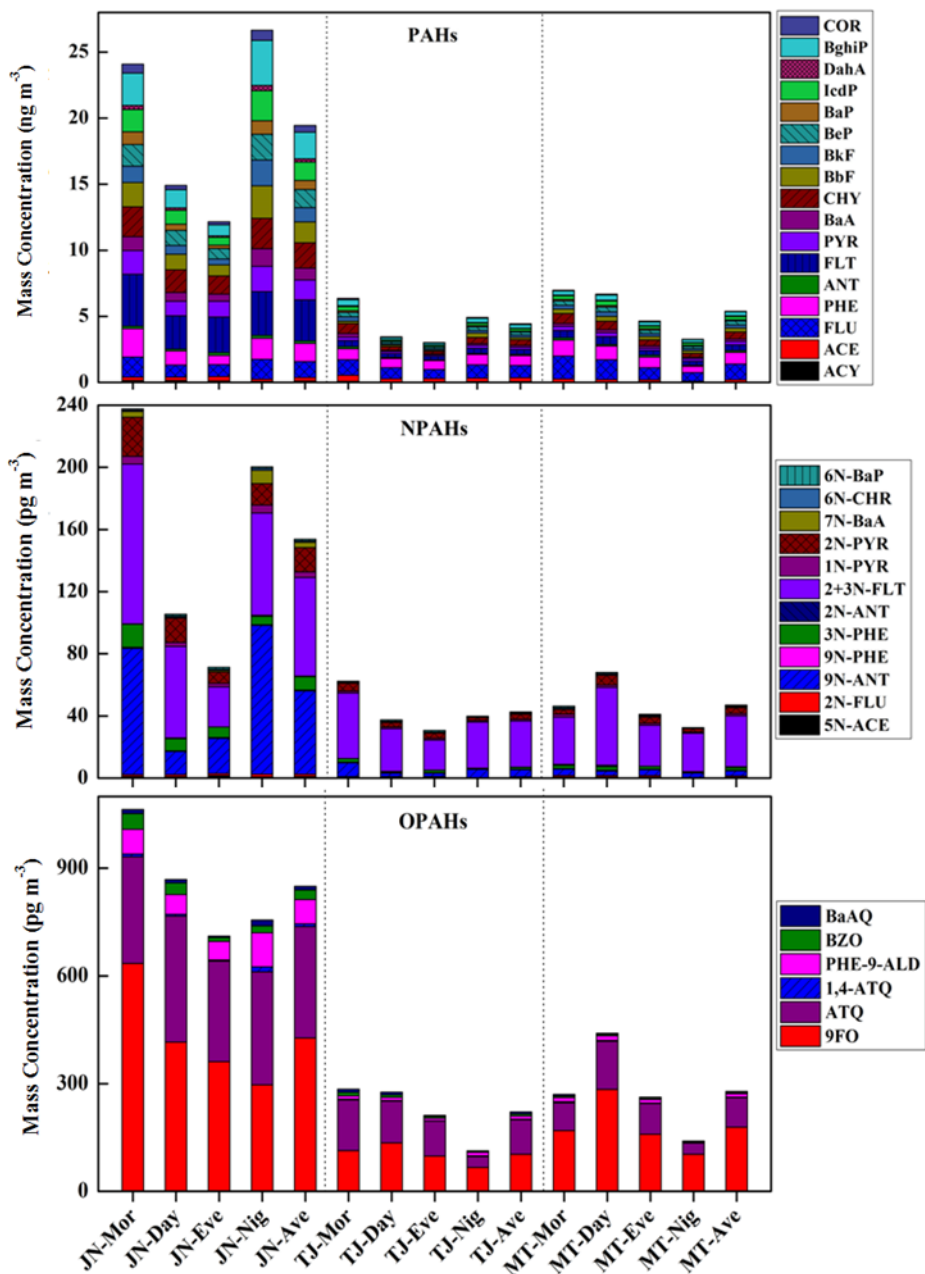
688 Zhuo, S., Du, W., Shen, G., Li, B., Liu, J., Cheng, H., 2017. Estimating relative contributions of
689 primary and secondary sources of ambient nitrated and oxygenated polycyclic aromatic
690 hydrocarbons. *Atmos. Environ.* 159, 126-134.

691 Zimmermann, K., Atkinson, R., Arey, J., Kojima, Y., Inazu, K., 2012. Isomer distributions of
692 molecular weight 247 and 273 nitro-PAHs in ambient samples, NIST diesel SRM, and
693 from radical-initiated chamber reactions. *Atmos. Environ.* 55, 431-439
694



695
696
697
698
699
700
701
702
703
704
705
706
707
708
709
710
711
712
713
714
715
716
717
718
719
720
721
722
723
724
725
726
727

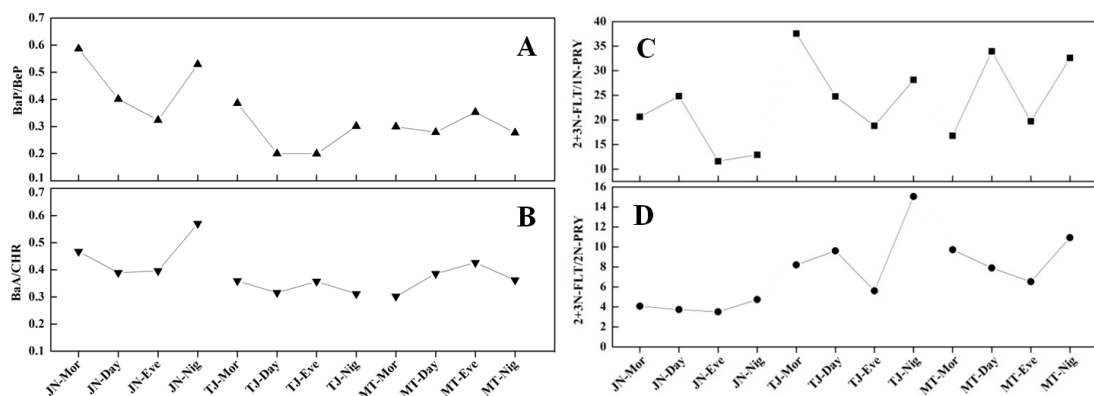
Fig. 1. The three sampling locations (Wang et al., 2009). The squares indicate background sampling sites.



728
 729
 730
 731
 732
 733
 734
 735
 736
 737
 738
 739
 740
 741

Fig. 2. Diurnal variation (Mor: morning, Eve: evening, Nig: night) and average (Ave) concentration of PAHs, NPAHs, and OPAHs at the urban (JN), marine (TJ) and mountain (MT) locations.

742

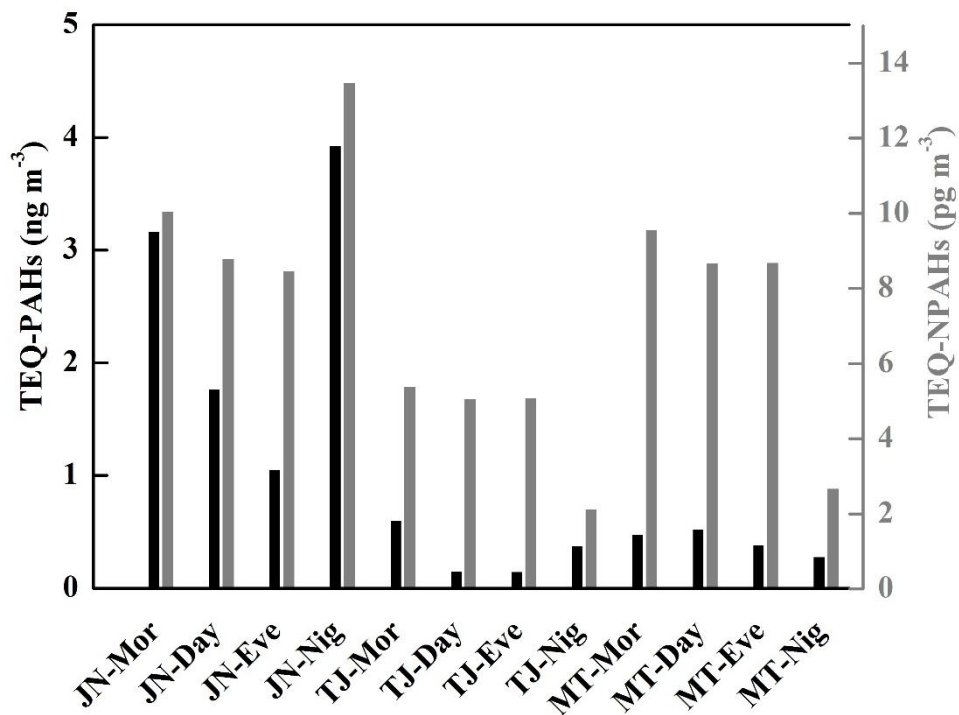


743

744

745 **Fig. 3.** Ratios of BaP/BeP (A), BaA/CHR (B), 2+3N-FLT/1N-PYR (C) and 2+3N-FLT/2N-PYR
 746 (D) at the three different sites during four sampling periods (Mor: morning, Eve: evening, Nig:
 747 night).

748



749

750 **Fig. 4.** TEQ of particulate PAHs and NPAHs during the four different sampling periods at the
 751 three locations.

752

753

754

755

756

757

758

Table 1

759

Diagnostic ratios of particulate PAHs at the three locations during the four sampling periods.

760

	FLT/(FLT+PYR)	IcdP/(IcdP+BghiP)
JN		
Morning	0.68	0.41
Day	0.70	0.43
Evening	0.70	0.41
Night	0.63	0.40
TJ		
Morning	0.66	0.39
Day	0.67	0.42
Evening	0.73	0.39
Night	0.66	0.37
MT		
Morning	0.65	0.47
Day	0.67	0.46
Evening	0.69	0.42
Night	0.63	0.45
Reference source emissions		
	>0.5 coal/ biomass combustion	>0.5 coal/ biomass combustion
	<0.5 and >0.4 petroleum combustion	<0.5 and >0.2 petroleum combustion
	<0.2 petroleum source	<0.2 petroleum source

761

762

763

764

765

766

767